

Synthesis and Characterization of Coconut Shell Waste-Based Graphene Oxide Composite with Nd₂O₃ via Solid-State Reaction

Muchlis

Laboratory of Materials Physics, Department of Physics, Universitas Negeri Makassar

Nurul Hanifah

Laboratory of Materials Physics, Department of Physics, Universitas Negeri Makassar

Indar Wahyuni Ilham

Laboratory of Materials Physics, Department of Physics, Universitas Negeri Makassar

Ayudiah Satria Ningsih

Laboratory of Materials Physics, Department of Physics, Universitas Negeri Makassar

他

<https://doi.org/10.5109/7326941>

出版情報 : Evergreen. 11 (4), pp.3005-3014, 2024-12. 九州大学グリーンテクノロジー研究教育センター

バージョン :

権利関係 : Creative Commons Attribution 4.0 International

Synthesis and Characterization of Coconut Shell Waste-Based Graphene Oxide Composite with Nd_2O_3 via Solid-State Reaction

Muchlis¹, Nurul Hanifah¹, Indar Wahyuni Ilham¹, Ayudiah Satria Ningsih¹, Vicran Zharvan¹, Samnur², Zurnansyah^{1,3}, Eko Hadi Sujiono^{1,*}

¹Laboratory of Materials Physics, Department of Physics, Universitas Negeri Makassar, Makassar, 90224, Indonesia.

²Department of Mechanical Engineering, Universitas Negeri Makassar, Makassar, 90224, Indonesia.

³Department of Physics, Universitas Gadjah Mada, Yogyakarta, 55281, Indonesia

*Author to whom correspondence should be addressed:

E-mail: e.h.sujiono@unm.ac.id

(Received September 12, 2023; Revised September 25, 2024; Accepted October 5, 2024).

Abstract: The 100 mesh and 400 mesh GO materials were synthesized from coconut shell waste-based graphite using the modified Hummer's method. These GO materials were then subjected to a calcination process at 950°C, during which they were reduced to reduced graphene oxide (rGO). The rGO was subsequently composited with Nd_2O_3 using a solid-state reaction method to obtain rGO-100 mesh/ Nd_2O_3 and rGO-400 mesh/ Nd_2O_3 materials. rGO-100 mesh/ Nd_2O_3 and rGO-400 mesh/ Nd_2O_3 were characterized using XRD, SEM-EDX, and FTIR. XRD analysis of rGO-100 mesh/ Nd_2O_3 and rGO-400 mesh/ Nd_2O_3 revealed a crystalline structure, with diffraction peaks corresponding to the Nd_2O_3 phase in the rGO/ Nd_2O_3 . FTIR spectra confirmed the presence of oxygen-containing functional groups, and the emergence of (Nd-O) groups in the rGO/ Nd_2O_3 , indicating the formation of the rGO/ Nd_2O_3 composite. The surface morphology of rGO/ Nd_2O_3 obtained from SEM characterization showed that Nd_2O_3 particles with varying particle sizes dominated the rGO/ Nd_2O_3 .

Keywords: Coconut Shell; Graphite; Graphene Oxide; Nd_2O_3 ; Solid-State Reaction

1. Introduction

Graphene is a material composed of a single two-dimensional layer of carbon atoms bonded together in a hexagonal structure^{1,2}, a promising material with high specific surface area, flexibility, electronic properties, conductivity, and good thermal stability³. This is what has made graphene highly popular for research in recent years. As a semimetal conductor, graphene and its derivatives have attracted significant interest in electronic research and applications, such as in energy storage supercapacitors, sensors, solar cell applications, and transparent conductive films, owing to their remarkable physical and chemical attributes^{4,5,6,7}.

Graphene is a single-layer 2D material composed of carbon with sp^2 hybridization. When subjected to oxidation, graphene oxide (GO) gives rise. GO stands as one of the derivatives of graphene⁸. GO is oxidized from graphite, which can be described as a carbon-based substance consisting of abundant oxygen-containing functional groups, commonly found at the edges of the GO structure. The electrical, optical, and chemical properties of GO are

similar to those of graphene. Moreover, GO has the advantage of being more cost-effective to produce and having a shorter production time than graphene⁹.

Environment-friendly precursors for producing graphene-based materials and their derivatives are gaining attention. Naturally, a variety of carbon sources exist, yet carbon extracted from mining substances is classified as non-renewable and environmentally unfriendly resources. On the other hand, carbon is also present in the shape of biomaterials obtained from plants, which is more environmentally friendly^{10,11,12}. Several previous studies have successfully synthesized graphite, GO, and reduced graphene oxide (rGO) from coconut shell waste^{13,14,15,16,17,18,19}. Furthermore, the incorporation of Nd_2O_3 into GO constitutes a research area that has been rarely explored. Among the diverse rare earth metal oxides, Neodymium Oxide (Nd_2O_3) possesses distinct applications owing to its unique catalytic properties, nanoscale surface, electrical characteristics, additive properties, and good doping attributes for enhancing the conductive/electronic capabilities of material²⁰. The properties of Nd_2O_3

particles are anticipated to enhance the attributes and characteristics of graphene and its biomass-based derivatives, thus potentially increasing the potential of biomass-based materials. In this study, the primary objective is to develop and evaluate a composite material by integrating GO derived from coconut shell waste with Nd_2O_3 . Specifically, the research aims to investigate the structural transformation of GO into reduced graphene oxide (rGO) during the solid-state synthesis process at 950°C , and evaluate how variations in GO mesh size (100 and 400 mesh) influence this transformation. Analyze the interaction between GO and Nd_2O_3 during the calcination process and its impact on the physical and chemical properties of the resulting composite. Characterize the obtained composites using XRD, SEM-EDX, and FTIR to confirm the formation and structural characteristics of the composites. By achieving these objectives, this study aims to contribute to the development of environmentally friendly graphene-based materials with enhanced properties for various applications.

2. Experimental Procedure

2.1 Materials

Hydrofluoric Acid (HF 40%), Sulfuric Acid (H_2SO_4), Potassium Permanganate (KMnO_4), Sodium Nitrate (NaNO_3), Hydrogen Peroxide (H_2O_2), and Neodymium Oxide (Nd_2O_3) (99.9%) of all materials used are Pro Analyst (PA) chemicals purchased from Sigma Aldrich.

2.2 Synthesis of Coconut Shell Waste-Based GO Composite with Nd_2O_3

In this study, the raw material for the production of graphene oxide (GO), namely graphite, was synthesized from coconut shell biomass waste using an optimization method as described in the research conducted by Sujiono et al., (2023)²¹. Subsequently, the produced graphite was oxidized to generate graphene oxide (GO) using a modified Hummers method based on the research conducted by Sujiono et al., (2020)¹⁹, where the precursor graphite's particle size was altered to 100 mesh and 400 mesh, subsequently labeled as GO-100 mesh and GO-400 mesh. Subsequently, a composite was synthesized by blending 1.5 grams of 100-mesh GO with 0.5 grams of Nd_2O_3 , followed by milling for 3 hours. The samples were then subjected to a heat treatment at 950°C for 6 hours for the calcination. During the calcination process, GO was reduced to rGO. The same procedure was carried out with 400-mesh GO. The two samples were labeled rGO-100 mesh/ Nd_2O_3 and rGO-400 mesh/ Nd_2O_3 .

2.3 Characterization

The crystalline phase composition of the sample was characterized by X-ray Diffraction (XRD) using a Shimadzu XRD 7000 Diffractometer (Shimadzu, Japan). The surface morphology and elements of the sample were characterized by Scanning Electron Microscopy-Energy

Dispersive X-ray (SEM-EDX) using a JSM-6510LA instrument. To identify functional groups of the sample, they were characterized by Fourier Transform Infra-Red (FTIR) Spectroscopy using a Thermo Scientific Nicolet iS10 instrument in the $4000\text{-}500\text{ cm}^{-1}$ with KBr pellets.

3. Results and Discussion

The crystal structure quality and orientation of the graphene oxide (GO) derived from coconut shell waste and the GO combined with Nd_2O_3 are illustrated in Fig. 1. The XRD pattern of GO in Fig. 1 (insert) exhibits an amorphous structure, yielding two prominent peaks at 2θ angles of approximately 23° and 43° , which correspond to the (002) and (001) planes, respectively^{22,23}. The peak at 2θ of approximately 23° may also be associated with the arrangement of graphene layers, which is typically uneven regarding the orientation of stacked graphene sheets¹⁰. Furthermore, the peak detected at around 43° , associated with the (001) plane, may indicate a reduction in oxygen functional groups and flaws within the sample, which might be further substantiated by FTIR analysis¹⁰. Before thermal treatment, the diffraction peaks at 23° and 43° suggest that the structure of GO contains disordered graphene layers and a minor reduction of oxygen functionalities, displaying characteristics identical to reduced graphene oxide (rGO), which may have experienced some reduction during the initial synthesis^{19,24}. However, after calcination at 950°C , both peaks disappear, indicating significant changes in the material's structure.

Figure 1 shows the XRD patterns of the rGO-100 mesh/ Nd_2O_3 and rGO-400 mesh/ Nd_2O_3 . According to the database, three phases have been identified in the rGO-100 mesh/ Nd_2O_3 sample. Firstly, the Nd_2O_3 phase was obtained, in accordance with the Powder Diffraction Pattern (PDF) No. 01-072-8425, appearing at 2θ angles of 26.84° , 29.74° , 30.76° , 40.49° , 47.41° , 53.42° , 56.98° , 64.07° , and 74.18° . The second phase identified was the H_3NdO_3 phase, corresponding to Crystallography Open Database (COD) No. 2106882, with peaks at 2θ angles of 15.92° , 27.76° , 28.73° , 32.16° , 36.85° , 40.37° , 42.99° , 48.62° , 49.10° , 51.49° , 59.91° , 65.38° , 71.59° and 78.79° . The third phase, Carbon (C), in accordance with PDF No. 01-075-0444, appeared at 2θ angles 26.31° , 46.50° , and 54.15° .

For rGO-400 mesh/ Nd_2O_3 , two phases were identified. Firstly, the Nd_2O_3 phase was obtained, in accordance with the Powder Diffraction Pattern (PDF) No. 01-072-8425, appearing at 2θ angles of 26.84° , 29.74° , 30.76° , 40.49° , 47.41° , 53.42° , 56.98° , 64.07° , and 74.18° . The second phase identified was the H_3NdO_3 phase, corresponding to Crystallography Open Database (COD) No. 2106882, with peaks at 2θ angles of 15.92° , 27.76° , 28.73° , 32.16° , 36.85° , 40.37° , 42.99° , 48.62° , 49.10° , 51.49° , 59.91° , 65.38° , 71.59° and 78.79° . The absence of the carbon phase in the rGO-400 mesh/ Nd_2O_3 is due to the reduction in particle size and the diminished carbon concentration following the calcination process, which results in peak broadening and

a decline in peak intensity, potentially rendering the peak undetectable relative to the prominent Nd_2O_3 peaks. As a result, the carbon diffraction peak becomes undetectable or difficult to interpret in the rGO-400 mesh/ Nd_2O_3 diffraction pattern^{25),26)}. Moreover, the rGO-100 mesh/ Nd_2O_3 and rGO-400 mesh/ Nd_2O_3 composites show the absence of characteristic rGO peaks in the XRD analysis. This absence is due to the dominance of the diffraction peaks from Nd_2O_3 , which overshadow the weaker diffraction signals from rGO. Specifically, the

crystal peaks of Nd_2O_3 tend to be sharper and more intense compared to the semi-amorphous peaks of rGO^{20),27)}. Furthermore, it is recognized that the synthesis procedure or thermal treatment can substantially influence the structure and properties of rGO^{19),24)}. The disappearance of these peaks may be attributed to the increased amorphous nature of graphene after calcination, where the interaction between graphene oxide and Nd_2O_3 disrupts the regularity of the graphene layers²⁸⁾. This transformation is consistent with the formation of rGO, as confirmed by FTIR results.

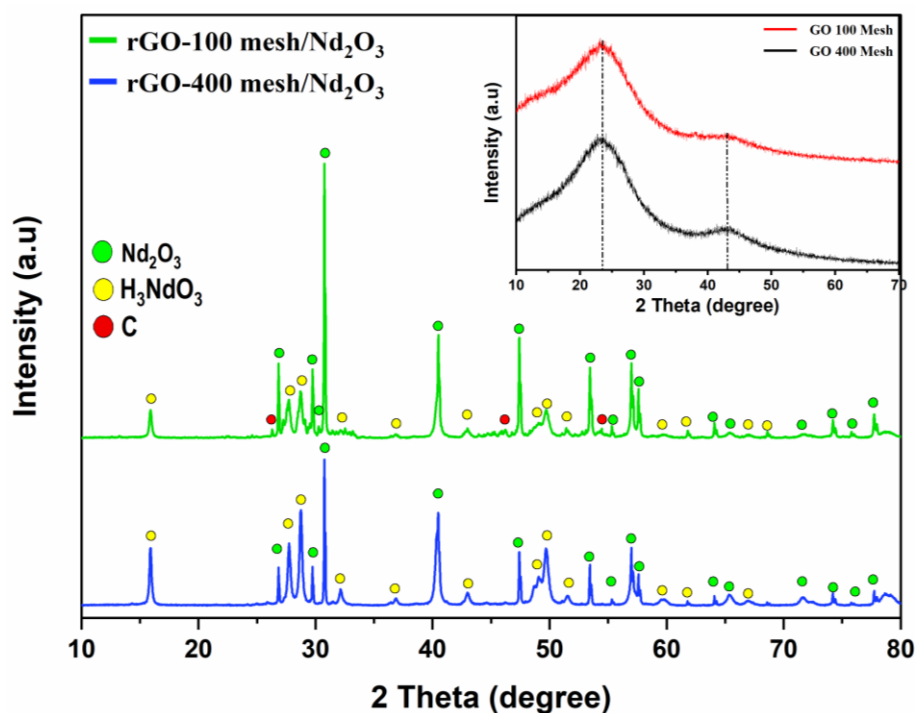


Fig. 1: Diffractogram pattern of rGO-100 mesh/ Nd_2O_3 and rGO-400 mesh/ Nd_2O_3 and **insert:** GO-100 mesh and GO-400 mesh based on coconut shell waste

Furthermore, FTIR was conducted to identify functional groups and describe the molecular structure of GO based on coconut shell waste graphite, as well as rGO/ Nd_2O_3 . From the FTIR spectrum of rGO 100-mesh and rGO 400-mesh, it can be discerned that patterns of interconnected carbon and oxygen functional groups have formed within the wavenumber range of 4000 cm^{-1} to 500 cm^{-1} . The spectrum of GO based on coconut shell waste, shown in Figure 2, exhibits a hydroxyl O–H group stretching

vibration band corresponding to the residual water intercalated between the GO sheets, the presence of carboxyl C=O and C–O and also stretching vibration of functional groups at the edge of the GO sheets carbonyl functional groups (–C=O). The absorption peak also relates to the epoxy C–OH stretching vibration band^{29),30)}. The comparison of functional groups between coconut shell waste-based GO and GO synthesized from commercial graphite can be observed in Table 1.

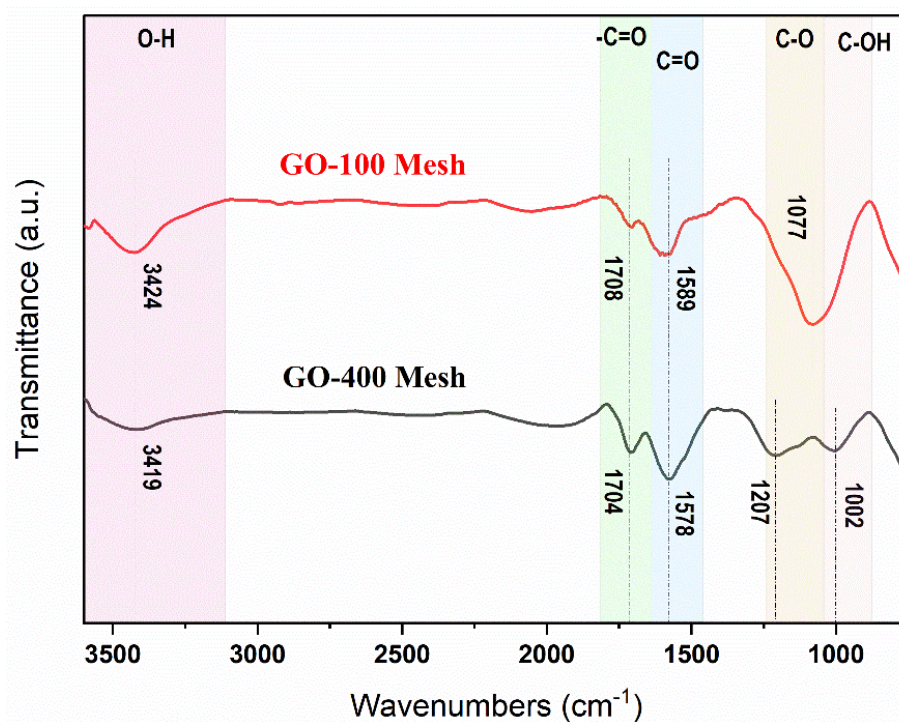


Fig. 2: FTIR spectrum of GO-100 mesh and GO-400 mesh based coconut shell

Table 1. Comparison of functional groups or bond types and wavenumbers of GO-based coconut shell waste with GO based commercial graphite³¹⁾.

Functional Groups	Wavenumbers (cm ⁻¹)		Functional Groups ³¹⁾	Wavenumbers (cm ⁻¹)
	GO-100 mesh	GO-400 mesh		
O – H	3424	3419	O – H	3414
-C = O	1708	1704	-C = O	1735
C = O	1589	1578	C = O	1556
C - O	-	1207	C – O	1248
C – OH	1077	1002	C – OH	1050

Figure 3 illustrates the absorption peak positions of rGO/Nd₂O₃ in the FTIR spectrum. The FTIR characterization results show significant changes in the chemical structure of graphene oxide (GO) after calcination at 950°C and the formation of a composite with Nd₂O₃. Before calcination, the FTIR spectrum exhibited a strong peak around 1500 cm⁻¹, corresponding to the vibration of C=O groups³¹⁾. This peak indicates a high concentration of oxygen-containing groups within the GO structure, a characteristic feature of this material³²⁾.

However, after the calcination process and the formation of the composite with Nd₂O₃, the intensity of the peak at 1500 cm⁻¹ drastically decreased. This reduction indicates that most oxygen-containing groups, particularly the C=O groups, were either removed or significantly diminished during calcination. This change is consistent with the transformation of GO into rGO, where the majority of oxygen groups are eliminated during the

calcination process^{33),34)}. A new peak emerged around 1600 cm⁻¹, corresponding to the vibration of carbon double bonds (C=C). The presence of this peak suggests that the graphitic structure of graphene begins to form after oxygen reduction, consistent with the formation of rGO. This C=C peak indicates that most oxygen bonds have been removed, and the resulting graphene has better carbon-carbon bond conjugation³⁵⁾. Meanwhile, new absorption peaks appear, indicating the formation of the rGO/Nd₂O₃ composite, particularly the Nd-O functional group^{36),37)}, and several new peaks have emerged, such as C–N, C≡C, and C=C=C^{30),38),39)}. In addition, new peaks related to oxygen groups in a different range after calcination were also detected, indicating the presence of additional oxygen groups formed due to the interaction between graphene and Nd₂O₃. These peaks suggest that although most of the oxygen has been reduced, the rGO/Nd₂O₃ composite retains some new oxygen groups, which may originate from the chemical

reaction between Nd₂O₃ and the residual oxygen groups in graphene oxide during the calcination process.

A comparison of bond types and wavenumbers between

rGO-100 mesh/Nd₂O₃ and rGO-400 mesh/Nd₂O₃ with those based on the literature is presented in **Table 2**.

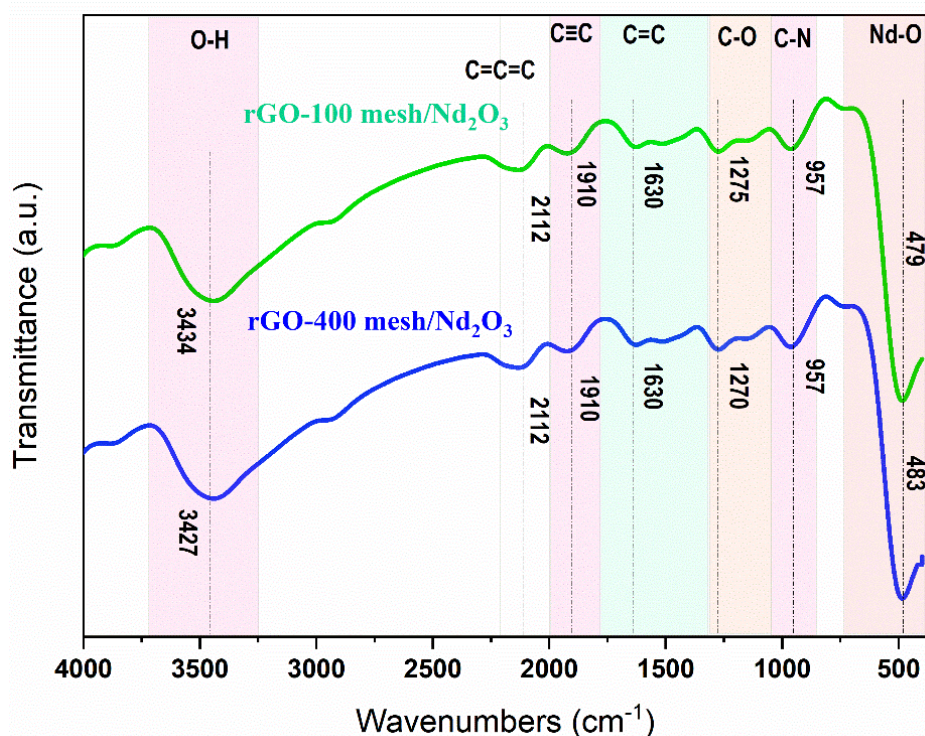


Fig. 3. FTIR spectrum of rGO-100 mesh/Nd₂O₃ and rGO-400 mesh/Nd₂O₃ based coconut shell waste

Table 2. A comparison of bond types and wave numbers of rGO/Nd₂O₃ with bond types and wave numbers based on literature.

Functional Groups	Wavenumbers (cm ⁻¹)		Functional Groups	Wavenumbers (cm ⁻¹)	Reference
	rGO-100 mesh /Nd ₂ O ₃	rGO-400 mesh /Nd ₂ O ₃			
O – H	3434	3427	O – H	3444	Sabir et al., ²⁰⁾
C=C=C	2112	2112	C=C=C	2190	Jehad et al., ³⁹⁾
C ≡ C	1910	1910	C ≡ C	1900	Jehad et al., ³⁹⁾
C = C	1630	1630	C = C	1620	Sabir et al., ²⁰⁾
C – O	1275	1279	C – O	1299	Sabir et al., ²⁰⁾
C – N	957	957	C – N	1034	Sabir et al., ²⁰⁾
Nd – O	479	480	Nd – O	411;533	Suhailath et al., ³⁶⁾

Subsequently, the surface morphology of the rGO/Nd₂O₃ after the calcination process was examined using SEM. Figure 4 shows the morphology and particle distribution between rGO-100 mesh/Nd₂O₃ (a,c,e) and rGO-400 mesh/Nd₂O₃ (b,d,f). It is observed that the morphology of the rGO/Nd₂O₃ forms particle structures, where the GO precursors with grain sizes of 100 mesh and

400 mesh exhibit granular-shaped particles characterized by a varied size distribution. The particle distribution on the surface of the rGO-100 mesh/Nd₂O₃ ranges from 0.1 μm to 0.90 μm, with an average of (0.48 ± 0.01) μm, and on the rGO-400 mesh/Nd₂O₃ from 0.15 μm to 0.60 μm, with an average of (0.44 ± 0.01) μm.

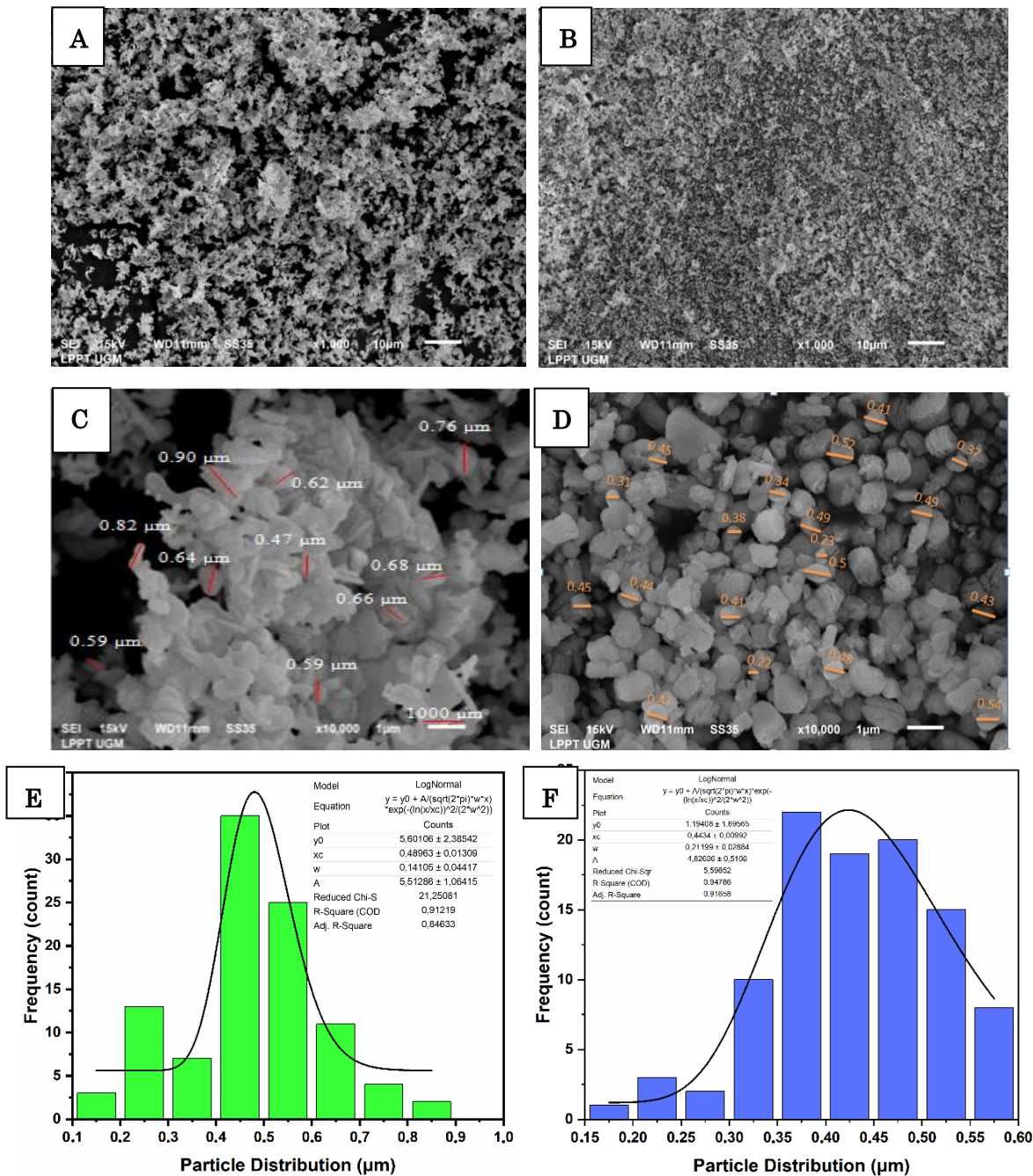


Fig. 4: Surface morphology and distribution particles of rGO-100 mesh/Nd₂O₃ (a,c,e) and rGO-400 mesh/Nd₂O₃ (b,d,f)

Differences in particle distribution between the rGO-100 mesh/Nd₂O₃ and rGO-400 mesh/Nd₂O₃ occur during calcination. The calcination process in both samples is assumed to significantly contribute to particle restructuring, affecting the size distribution after the calcination process. Additionally, differences in the initial precursor grain size of the GO are considered a significant factor in providing a different foundation for particle growth during the synthesis stage, creating variation in particle distribution between the two samples⁴⁰. Although SEM images may not reveal significant morphological differences between rGO and Nd₂O₃, the particle size measurements encompass dimensions and distribution closely associated with the

morphological structure. Furthermore, additional characterization, such as EDX analysis and mapping, provide further confirmation regarding the chemical differences and distribution of composite elements between rGO and Nd₂O₃ in the samples.

The EDX elemental mapping, as depicted in Fig. 5 and detailed in Table 3, illustrates the percentage ratios of Nd, O, and C elements after the synthesis process at a calcination temperature of 900°C. This indicates differences in carbon content between the rGO-100 mesh/Nd₂O₃ and rGO-400 mesh/Nd₂O₃ composites. This might be attributed to differences in the grain size of GO; a smaller grain size in rGO-400 mesh/Nd₂O₃ results in a

larger surface area compared to rGO-100 mesh/Nd₂O₃. This has the potential to influence reactivity and combustion ease during the calcination process in rGO-400 mesh/Nd₂O₃, thus reducing the presence of remaining carbon elements⁴⁰.

Figure 5 also displays EDX analysis and elemental maps of the rGO-100 mesh/Nd₂O₃ (a,b,c,g) and rGO-400 mesh/Nd₂O₃ (d,e,f,h), demonstrating variations in carbon content. These differences are attributed to the diverse

grain sizes in the GO before combining with Nd₂O₃. Therefore, during the calcination process, larger grain sizes will retain a higher amount of carbon elements⁴⁰. This supports the previous SEM and XRD regarding the formation of a composite between rGO and Nd₂O₃, which, although it may not be apparent at the particle morphology level, can be identified through more in-depth chemical analysis.

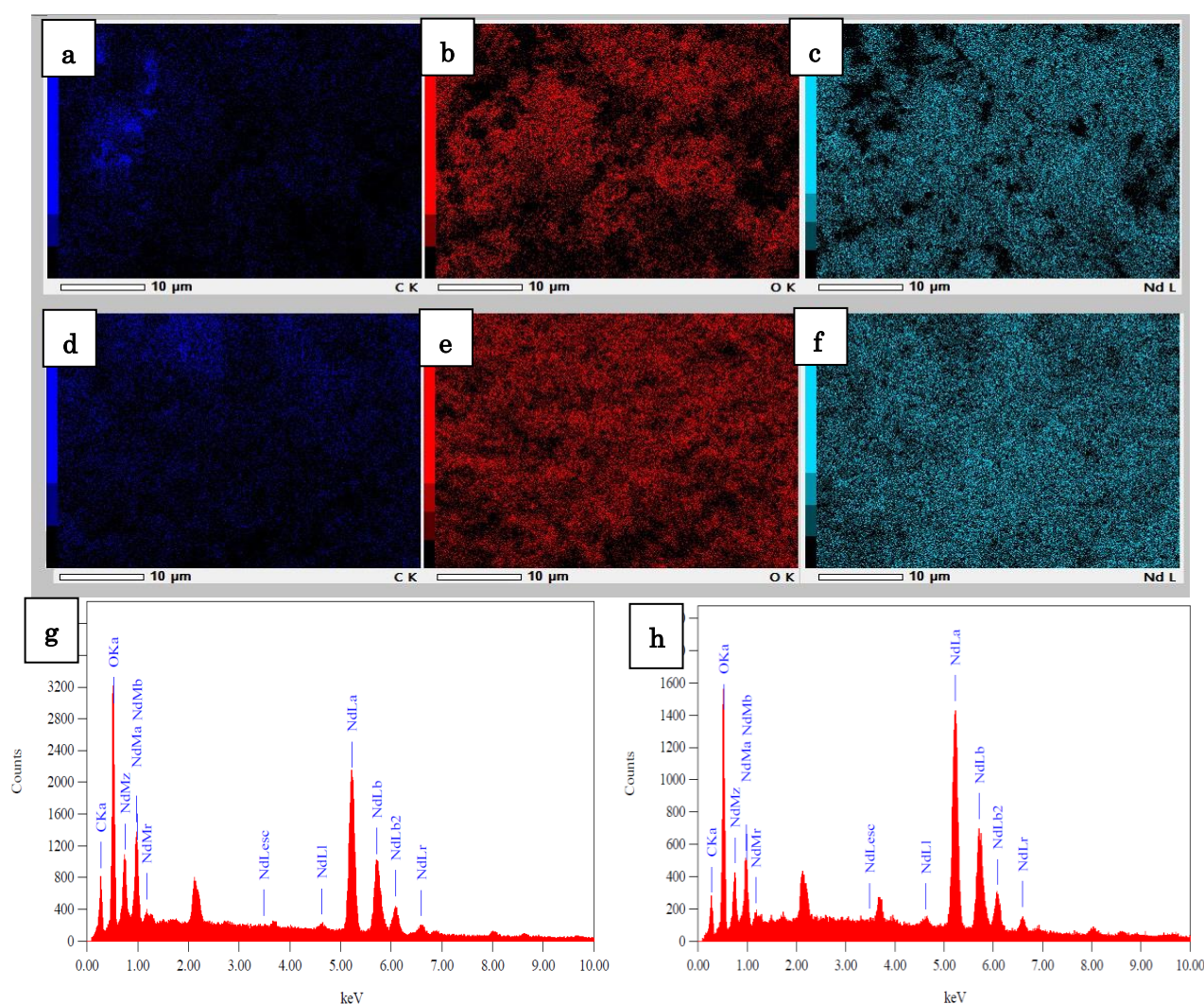


Fig. 5: The element map surface area of (a,b,c) rGO-100 mesh/Nd₂O₃ (d,e,f) rGO-400 mesh/Nd₂O₃ (g) EDX rGO-100 mesh/Nd₂O₃ and (h) EDX rGO-400 mesh/Nd₂O₃

Table 3. EDX percentage of elements present in rGO-100 mesh/Nd₂O₃ and rGO-400 mesh/Nd₂O₃

Name	Elements	Mass%	Atom%
rGO-100 mesh/Nd ₂ O ₃	C	8.78	28.25
	O	22.02	53.20
	Nd	69.20	15.54
rGO-400 mesh/Nd ₂ O ₃	C	5.05	20.73
	O	17.06	52.62
	Nd	77.89	26.65

4. Conclusion

GO-100 mesh and GO-400 mesh have been successfully synthesized using a modified Hummer's method, and rGO-100 mesh/Nd₂O₃ and rGO-400 mesh/Nd₂O₃ have been successfully synthesized using a solid-state reaction method. XRD analysis indicates a crystalline structure with diffraction peak formation of Nd₂O₃ and H₃NdO₃ phase for the GO-400 mesh/Nd₂O₃, and for the GO-100 mesh/Nd₂O₃, phases Nd₂O₃, H₃NdO₃, and Carbon (C) are formed. The FTIR spectrum of GO confirms the presence of oxygen compound functional groups, namely O–H group stretching vibration band, carboxyl C=O, C–O, stretching vibration of carbonyl functional groups (–C=O) and also epoxy C–OH stretching vibration band, which are characteristic features of the graphene oxide spectrum. Meanwhile, the FTIR spectrum for rGO-100 mesh/Nd₂O₃ and rGO-400 mesh/Nd₂O₃ shows several new absorption peaks, such as a C=C peak, indicating that most oxygen bonds have been removed. The resulting graphene has better carbon-carbon bond conjugation, C=C=C, C≡C, C–N, and Nd–O, indicating the formation of functional groups of Nd₂O₃ in the sample. Furthermore, the surface morphology of rGO/Nd₂O₃ obtained from SEM-EDX characterization reveals that the rGO/Nd₂O₃ has been successfully produced but is still dominated by Nd₂O₃ particles.

Acknowledgments

This work was supported by the fundamental research program, The Directorate of Research, Technology, and Community Services, Directorate General of Higher Education, Research and Technology, Ministry of Education, Culture, Research and Technology, Republic of Indonesia, under contract number: 065/E5/PG.02.00.PL/2024 and the Universitas Negeri Makassar Research Institution, a research scheme of PNBP Majelis Profesor under contract number: 1290/UN36.11/LP2M/2024.

References

- 1) X. Mei, and J. Ouyang, "Ultrasonication-assisted ultrafast reduction of graphene oxide by zinc powder at room temperature," *Carbon*, **49** (15) 5389–5397 (2011). doi:10.1016/j.carbon.2011.08.019.
- 2) S. Pei, and H.M. Cheng, "The reduction of graphene oxide," *Carbon*, **50** (9) 3210–3228 (2012). doi:10.1016/j.carbon.2011.11.010.
- 3) Y. Li, Y. Zhao, Y. Chen, Y. Chen, D. Zhou, and Z. Zhao, "Direct synthesis of single-layer graphene films on quartz substrate by a nanoparticle-assisted method," *Applied Surface Science*, **529** (June) 147082 (2020). doi:10.1016/j.apsusc.2020.147082.
- 4) H.J. Kil, K. Yun, M.E. Yoo, S. Kim, and J.W. Park, "Solution-processed graphene oxide electrode for supercapacitors fabricated using low temperature thermal reduction," *RSC Advances*, **10** (37) 22102–22111 (2020). doi:10.1039/d0ra03985c.
- 5) N. Sharma, R. Vyas, V. Sharma, H. Rahman, S.K. Sharma, and K. Sachdev, "A comparative study on gas-sensing behavior of reduced graphene oxide (rGO) synthesized by chemical and environment-friendly green method," *Appl Nanosci*, **10** (2) 517–528 (2020). doi:10.1007/s13204-019-01138-7.
- 6) A. Capasso, L. Salamandra, G. Faggio, T. Dikonimos, F. Buonocore, V. Morandi, L. Ortolani, and N. Lisi, "Chemical vapor deposited graphene-based derivative as high-performance hole transport material for organic photovoltaics," *ACS Appl. Mater. Interfaces*, **8** (36) 23844–23853 (2016). doi:10.1021/acsami.6b06749.
- 7) X. Fan, Z. Zhao, X. Liang, X. Huai, C. Wang, J. Liu, and C. Duan, "Graphene reinforced anticorrosion transparent conductive composite film based on ultrathin ag nanofilm," *Materials*, **15** (14) 4802 (2022). doi:10.3390/ma15144802.
- 8) D. Panda, A. Nandi, S.K. Datta, H. Saha, and S. Majumdar, "Selective detection of carbon monoxide (CO) gas by reduced graphene oxide (rGO) at room temperature," *RSC Adv*, **6** (53) 47337–47348 (2016). doi:10.1039/C6RA06058G.
- 9) Y.F. Li, Y.Z. Liu, W.K. Zhang, C.Y. Guo, and C.M. Chen, "Green synthesis of reduced graphene oxide paper using Zn powder for supercapacitors," *Materials Letters*, **157** 273–276 (2015). doi:10.1016/j.matlet.2015.05.114.
- 10) D. Ristiani, R. Asih, F. Astuti, M.A. Baqiya, C. Kaewhan, S. Tunmee, H. Nakajima, S. Soontaranon, and Darminto, "Mesostructural study on graphenic-based carbon prepared from coconut shells by heat treatment and liquid exfoliation," *Heliyon*, **8** (3) e09032 (2022). doi:10.1016/j.heliyon.2022.e09032.
- 11) Rabi K Ahmad, Shaharin A Sulaiman, M Amin B A Majid, S. Yusuf, Sharul S Dol, M. Inayat, and Hadiza A Umar, "Assessing the technical and environmental potential of coconut shell biomass: experimental study through pyrolysis and gasification," *Evergreen*, **10** (1) 585–593 (2023). doi:10.5109/6782165.
- 12) J. Waluyo, Muhammad Muadz Setianto, Nadiya Rizki Safitri, Sunu Herwi Pranolo, Ari Diana Susanti, Margono, and Paryanto, "Characterization of biochar briquettes from coconut shell with the effect of binder: molasses, cow manure and horse manure," *Evergreen*, **10** (1) 539–545 (2023). doi:10.5109/6782158.
- 13) G. Supriyanto, N.K. Rukman, A.K. Nisa, M. Jannatin, B. Piere, Abdullah, M.Z. Fahmi, and H.S. Kusuma, "Graphene oxide from Indonesian biomass: synthesis and characterization," *BioResources*, **13** (3) 4832–4840 (2018). doi:10.15376/biores.13.3.4832-4840.
- 14) G.B.A. Putra, H.Y. Pradana, D.E.T. Soenaryo, M.A. Baqiya, and Darminto, "Synthesis of green Fe₃+/glucose/rGO electrode for supercapacitor

- application assisted by chemical exfoliation process from burning coconut shell,” in: Surabaya, Indonesia, 2018: p. 020040. doi:10.1063/1.5030262.
- 15) R. Asih, M.M. Septya, E.B. Yutomo, F. Astuti, M.A. Baqiya, and D. Darminto, “Physical properties comparison of rgo-like phase prepared from coconut shell and the commercial product,” *Jurnal Fisika Dan Aplikasinya*, **16** (2) 82 (2020). doi:10.12962/j24604682.v16i2.6712.
- 16) D. Ristiani, R. Asih, N.S. Puspitasari, M.A. Baqiya, Risdiana, M. Kato, Y. Koike, S. Yamaguchi, Y. Furukawa, and Darminto, “Introduction of na⁺ in reduced graphene oxide prepared from coconut shells and its magnetic properties,” *IEEE Trans. Magn.*, **56** (7) 1–6 (2020). doi:10.1109/TMAG.2020.2994175.
- 17) Samnur, N. Azizah, N. Fahira, Zurnansyah, D. Zabrian, V. Zharvan, and E.H. Sujiono, “Comparative study and characterization of reduced graphene oxide (rgo) and porous reduced graphene oxide (p-rgo) based on coconut shell waste,” *Journal of Nano- and Electronic Physics*, **13** (6) 1–6 (2021). doi:10.21272/JNEP.13(6).06017.
- 18) A.M. Afdhal Saputra, N. Agustina, A. -, Z. -, S. -, and E.H. Sujiono, “Synthesis and characterisation of graphene oxide/chitosan composite membranes from natural waste,” *JPS*, **33** (3) 63–79 (2022). doi:10.21315/jps2022.33.3.5.
- 19) E.H. Sujiono, Zurnansyah, D. Zabrian, M.Y. Dahlan, B.D. Amin, Samnur, and J. Agus, “Graphene oxide based coconut shell waste: synthesis by modified hummers method and characterization,” *Heliyon*, **6** (8) e04568 (2020). doi:10.1016/j.heliyon.2020.e04568.
- 20) Z. Sabir, M. Akhtar, S. Zulfiqar, S. Zafar, P.O. Agboola, S. Haider, S.A. Ragab, M.F. Warsi, and I. Shakir, “L-cysteine functionalized nd2o3/rgo modified glassy carbon electrode: a new sensing strategy for the rapid, sensitive and simultaneous detection of toxic nitrophenol isomers,” *Synthetic Metals*, **277** 116774 (2021). doi:10.1016/j.synthmet.2021.116774.
- 21) E.H. Sujiono, A.M.A. Saputra, Muchlis, B.D. Usman, N. Fadilah, Zurnansyah, D. Zabrian, N. Azizah, and Samnur, “Coconut shell waste-derived graphene oxide composite with neodymium oxide (nd2o3) for advanced applications,” *Results in Materials*, **20** 100480 (2023). doi:10.1016/j.rinma.2023.100480.
- 22) D.A. Acevedo-Guzmán, L. Huerta, M. Bizarro, V. Meza-Laguna, P. Rudolf, V.A. Basiuk, and E.V. Basiuk, “Solvothermal synthesis of lanthanide-functionalized graphene oxide nanocomposites,” *Materials Chemistry and Physics*, **304** 127840 (2023). doi:10.1016/j.matchemphys.2023.127840.
- 23) Atmanto Heru Wibowo, Husen Al Arraf, A. Masykur, F. Rahmawati, M. Firdaus, F. Pasila, U. Farahdina, and N. Nasori, “Composite of polyaniline/reduced graphene oxide with the single-, bi- and tri- metal oxides modification and the effect on the capacitance properties,” *Evergreen*, **10** (1) 85–93 (2023). doi:10.5109/6781053.
- 24) P. Das, A.B. Deoghare, and S.R. Maity, “A novel approach to synthesise reduced graphene oxide (rgo) at low thermal conditions,” *Arab J Sci Eng*, **46** (6) 5467–5475 (2021). doi:10.1007/s13369-020-04956-y.
- 25) M. Ermrich, and D. Opper, “XRD for the analyst: getting acquainted with the principles,” 2nd revised edition, PANalytical, Almelo, 2013.
- 26) N.F. Yusoff, Z. Jamil, and N. Osman, “The influence of calcination temperature on crystallographic and chemical characteristics of nio-ceo₂ powder for pcfc anodes,” *IOP Conf. Ser.: Earth Environ. Sci.*, **1151** (1) 012050 (2023). doi:10.1088/1755-1315/1151/1/012050.
- 27) L. Zheng, Z. Zhu, Y. Kuai, Q. Huang, M. Zhang, Y. Wang, and A. Li, “Modification of separators with neodymium oxide/graphene composite to enhance lithium-sulfur battery performance,” *Journal of Rare Earths*, S1002072123002454 (2023). doi:10.1016/j.jre.2023.09.006.
- 28) A. Wanag, E. Kusiak-Nejman, A. Czyżewski, D. Moszyński, and A.W. Morawski, “Influence of rgo and preparation method on the physicochemical and photocatalytic properties of tio2/reduced graphene oxide photocatalysts,” *Catalysis*, **11** (11) 1333 (2021). doi:10.3390/catal11111333.
- 29) M. Ebrahimi Naghani, M. Neghabi, M. Zadsar, and H. Abbastabar Ahangar, “Synthesis and characterization of linear/nonlinear optical properties of graphene oxide and reduced graphene oxide-based zinc oxide nanocomposite,” *Sci Rep*, **13** (1) 1496 (2023). doi:10.1038/s41598-023-28307-7.
- 30) J. Coates, “Interpretation of Infrared Spectra, A Practical Approach,” in: R.A. Meyers (Ed.), *Encyclopedia of Analytical Chemistry*, 1st ed., Wiley, 2000. doi:10.1002/9780470027318.a5606.
- 31) R.J. Kadhim, F.H. Al-Ani, M. Al-shaeli, Q.F. Alsahly, and A. Figoli, “Removal of dyes using graphene oxide (go) mixed matrix membranes,” *Membranes*, **10** (12) 366 (2020). doi:10.3390/membranes10120366.
- 32) D.Yu. Kornilov, and S.P. Gubin, “Graphene oxide: structure, properties, synthesis, and reduction (a review),” *Russ. J. Inorg. Chem.*, **65** (13) 1965–1976 (2020). doi:10.1134/S0036023620130021.
- 33) I.O. Faniyi, O. Fasakin, B. Olofinjana, A.S. Adekunle, T.V. Oluwasusi, M.A. Eleruja, and E.O.B. Ajayi, “The comparative analyses of reduced graphene oxide (rgo) prepared via green, mild and chemical approaches,” *SN Appl. Sci.*, **1** (10) 1181 (2019). doi:10.1007/s42452-019-1188-7.
- 34) A.A. Ismail, R.A. Geioushy, H. Bouzid, S.A. Al-Sayari, A. Al-Hajry, and D.W. Bahnemann, “TiO₂ decoration of graphene layers for highly efficient photocatalyst: impact of calcination at different gas atmosphere on photocatalytic efficiency,” *Applied Catalysis B: Environmental*, **129** 62–70 (2013). doi:10.1016/j.apcatb.2012.09.024.

- 35) A. Mahmud, and A.B. Deoghare, "A comparative study on coconut shell-derived graphene oxide and reduced graphene oxide," *Current Applied Physics*, **62** 12–21 (2024). doi:10.1016/j.cap.2024.03.009.
- 36) K. Suhailath, B.K. Bahuleyan, and M.T. Ramesan, "Synthesis, characterization, thermal properties and temperature-dependent ac conductivity studies of poly (butyl methacrylate)/neodymium oxide nanocomposites," *J Inorg Organomet Polym*, **31** (1) 365–374 (2021). doi:10.1007/s10904-020-01665-9.
- 37) R. Yuvakkumar, and S.I. Hong, "Nd₂O₃: novel synthesis and characterization," *J Sol-Gel Sci Technol*, **73** (2) 511–517 (2015). doi:10.1007/s10971-015-3629-0.
- 38) A.B.D. Nandiyanto, R. Oktiani, and R. Ragadhita, "How to read and interpret ftir spectroscopy of organic material," *Indonesian J. Sci. Technol*, **4** (1) 97 (2019). doi:10.17509/ijost.v4i1.15806.
- 39) A.K. Jehad, K. Kocabas, and M. Yurddaskal, "A comparative study for producing few-layer graphene sheets via electrochemical and microwave-assisted exfoliation from graphite powder," *J Mater Sci: Mater Electron*, **31** (9) 7022–7034 (2020). doi:10.1007/s10854-020-03268-z.
- 40) E. Picheau, S. Amar, A. Derré, A. Pénicaud, and F. Hof, "An introduction to the combustion of carbon materials," *Chemistry A European J*, **28** (54) e202200117 (2022). doi:10.1002/chem.202200117.